Corneal Epithelium–Derived Netrin-1 Alleviates Dry Eye Disease via Regulating Dendritic Cell Activation

Chaoqun Yu,[1] Peng Chen,[2] Jing Xu,[1] Susu Wei,[1] Qilong Cao,[3] Chuanlong Guo,[4] Xianggen Wu,[4] and Guohu Di[1]

[1]Department of Special Medicine, School of Basic Medicine, Qingdao University, Qingdao, China
[2]Department of Anthropotomy and Histo-Embryology, School of Basic Medicine, Qingdao University, Qingdao, China
[3]Qingdao Haier Biotech Co. Ltd., Qingdao, China
[4]College of Chemical Engineering, Qingdao University of Science and Technology, Qingdao, China

Correspondence: Guohu Di, Qingdao University, 308 Ningxia Road, Qingdao 266071, China; diguohu@qdu.edu.cn.

CY and PC contributed equally to this work.

Received: August 30, 2021
Accepted: May 16, 2022
Published: June 1, 2022

Citation: Yu C, Chen P, Xu J, et al. Corneal epithelium–derived netrin-1 alleviates dry eye disease via regulating dendritic cell activation. *Invest Ophthalmol Vis Sci.* 2022;63(6):1. https://doi.org/10.1167/iovs.63.6.1

Purpose. To investigate the expression of corneal epithelium–derived netrin-1 (NTN-1) and its immunoregulatory function in dry eye disease (DED) using a DED mouse model.

Methods. We generated DED mouse models with desiccating stress under scopolamine treatment. RNA sequencing was performed to identify differentially expressed genes (DEGs) in the corneal epithelium of DED mice. NTN-1 expression was analyzed via real-time PCR, immunofluorescence staining, and immunoblotting. The DED mice were then treated with recombinant NTN-1 or neutralizing antibodies to investigate the severity of the disease, dendritic cell (DC) activation, and inflammatory cytokine expression.

Results. A total of 347 DEGs (292 upregulated and 55 downregulated) were identified in the corneal epithelium of DED mice: corneal epithelium–derived NTN-1 expression was significantly decreased in DED mice compared to that in control mice. Topical recombinant NTN-1 application alleviated the severity of the disease, accompanied by restoration of tear secretion and goblet cell density. In addition, NTN-1 decreased the number of DCs, inhibited the activation of the DCs and Th17 cells, and reduced the expression of inflammatory factors in DED mice. In contrast, blocking endogenous NTN-1 activity with an anti–NTN-1 antibody aggravated the disease, enhanced DC activation, and upregulated the inflammatory factors in the conjunctivae of DED mice.

Conclusions. We identified decreased NTN-1 expression in the corneal epithelium of DED mice. Our findings elucidate the role of NTN-1 in alleviating DED and impeding DC activation, thereby indicating its therapeutic potential in suppressing ocular inflammation in DED.

Keywords: dry eye disease, netrin-1, corneal epithelium, dendritic cells, Th17 cells

Dry eye disease (DED) is a chronic progressive ocular surface disease caused by multiple factors that lead to a variety of symptoms, including eye burn, pain, vision loss, and photophobia.[1] DED affects 5% to 35% of the general population and has a significant impact on the overall quality of life.[2] Although DED is a complex multifactorial disease, increasing evidence shows that ocular surface inflammation plays a key role in the pathologic progression of the disease.[3]

In recent years, increasing studies have been focused on neuroimmune interactions; dendritic cells (DCs) are key to these interactions.[4,5] DC, an antigen-presenting cell (APC), constitutes the main immune cell population in the corneal epithelium and can interact with sensory nerves.[6–8] Under homeostatic conditions, the expression of major histocompatibility complex class II (MHC-II) and cluster of differentiation 86 (CD86) in immature DCs is very low.[9] The DCs undergo maturation during DED.[10] Mature DCs with high MHC-II and CD86 expression activate immature T cells, resulting in the activation of effector T cells,[11] including T helper 17 (Th17) cells.[12,13] Previous studies have demonstrated the important pathogenic role of Th17 cells in DED.[14–16] Cytokines secreted by Th17 cells, such as IL-17, IFN-γ, and IL-1β, destroy the corneal barrier and lead to persistent inflammation.[17–19] However, immunomodulatory factors synthesized by the corneal epithelium, such as programed death ligand 1 (PD-L1),[20] pigment epithelium–derived factor (PEDF),[21] and thrombospondin-1 (TSP-1),[22] can impede DED pathogenesis by regulating the immune response.

Netrin-1 (NTN-1) is a 67-kDa laminin-related secretory protein belonging to the netrin family. NTN-1 was originally described as a "guiding clue" that affects axon migration during the development of the central nervous system.[23] In addition to its expression in the nervous system, NTN-1 is also widely expressed in other tissues, such as the intestinal epithelium, lungs, and breast.[24] Besides the regulatory role of axonal elongation and orientation, recent studies have found that NTN-1 is a negative guiding signal of leukocyte migration, indicating that NTN-1 has an anti-inflammatory effect.[24] It has been proved that NTN-1 plays

an anti-inflammatory role in peritonitis, experimental colitis, and lung injury.[25–27] Also, NTN-1 is expressed in corneal tissue, predominantly in the corneal epithelium.[28–30] NTN-1 has been reported to treat various ocular diseases. In a rat model with ocular alkali burn, NTN-1 could inhibit alkali burn–induced inflammation and angiogenesis.[28] In hyperglycemic mouse models, NTN-1 promoted the proliferation and migration of corneal epithelial cells, as well as the healing of diabetic corneal wounds.[30]

Based on the multiple functions of NTN-1 and the pathogenic characteristics of DED, we speculate that NTN-1 may have therapeutic potential in DED treatment. In this study, we have discussed the therapeutic effects of NTN-1 in DED mice. Furthermore, the inhibitory effects of NTN-1 on DC maturation and its anti-inflammatory effects have also been discussed.

Materials and Methods

Animal Model

Female C57BL/6 mice (6–8 weeks old) were purchased from Jinan Pengyue Experimental Animal Breeding Co. Ltd. (Jinan, Shandong, China). All animal experiments were approved by the Experimental Animal Ethics Committee of Qingdao University and conformed to the standards of the ARVO Statement for the Use of Animals in Ophthalmic and Vision Research. DED was induced in the mice subcutaneously via scopolamine injection and exposure to a desiccating environment, as described previously.[31] Briefly, mice received subcutaneous injections of scopolamine hydrobromide (0.5 mg/0.2 mL; Meilubio, Dalian, China) four times a day (at 8:00 a.m., 11:00 a.m., 2:00 p.m., and 5:00 p.m.) and were housed in a chamber (ambient relative humidity $\leq$30% and temperature = 22 $\pm$ 1°C) with a fan (2.5 $\pm$ 0.5 m/s) for 5 consecutive days. Age- and sex-matched mice placed in a standard environment served as the control.

Topical Administration of Recombinant Mouse NTN-1 and Anti-Mouse NTN-1 Antibody

To investigate the anti-inflammatory effects of NTN-1, DED mice were randomly categorized into four groups (five mice per group): the first three groups received 25 ng/5 µL recombinant mouse NTN-1 (1109-N1; R&D, Minneapolis, MN, USA), 250 ng/5 µL anti-mouse NTN-1 antibody (R&D, AF1109), or 250 ng/5 µL goat IgG (R&D, AB-108-C), and mice in the control group received PBS. The mice in each group received 5 µL of corresponding medication via ocular surface instillation four times daily (at 8:00 a.m., 11:00 a.m., 2:00 p.m., and 5:00 p.m.) for 5 consecutive days during the entire course of DED induction.

RNA Sequencing and Data Analysis

For RNA sequencing (RNA-seq), corneal epithelium of a control mouse and DED mouse (corneal epithelium of four eyes was pooled together as a sample) was collected using Algerbrush II (The Alger Company, Lago Vista, TX, USA) under a stereomicroscope (SZ51; Olympus, Tokyo, Japan), and total RNAs were extracted. Sequencing cDNA libraries were prepared using a NEBNext Ultra RNA Library Prep Kit (Illumina, San Diego, CA, USA). RNA-seq analysis was performed by Personal Biotechnology Co. Ltd. (Shanghai, China). The reads containing adaptors with 3′ ends, which are low-quality reads, were filtered from the raw reads to obtain clean reads. Clean reads were aligned with the reference genome using HISAT2 (2.0.5) software. The read count was aligned with each gene using HTseq as the raw expression of the gene, and then, the expression was normalized with fragments per kilobases per million fragments. Differential gene expression analyses were performed with DEseq. Genes with the absolute value of $\log_2$(fold change) >1 and $P < 0.05$ were defined as differentially expressed genes (DEGs). Volcano plots of DEGs were obtained using the ggplot2 R package. Cluster analysis was performed using the Pheatmap R package. Kyoto Encyclopedia of Genes and Genomes (KEGG) pathway analyses of DEGs were performed using a clusterProfiler.

Western Blot Analysis

The total protein was extracted from corneal epithelium as described previously.[32] The quantified and denatured total proteins were separated by 10% SDS-PAGE and then transferred electronically to polyvinylidene fluoride membranes (Millipore, Bedford, MA, USA). Thereafter, the blots were blocked in 5% milk-Tris-buffered saline containing 0.1% Tween-20 for 1 hour and then incubated with primary antibodies (anti–NTN-1 antibody [1:1000; ab126729, Abcam, Cambridge, MA, USA] and anti-GAPDH antibody [1:3000; KC-5G5, Kangcheng, Shanghai, China]) at 4°C overnight. The following day, the membranes were incubated with HRP-conjugated goat anti-rabbit IgG (1:5000, ZB-2301; ZSGB-BIO, Beijing, China) for 1 hour at room temperature. An ECL kit (P1050-250; Applygen, Beijing, China) was used for detection.

Immunofluorescent Staining

Samples were collected and cut into frozen sections as described previously.[33] The frozen corneal sections (7 µm thick) were fixed in 4% paraformaldehyde (PFA) for 20 minutes, rehydrated with PBS, and permeabilized in 0.1% Triton X-100 (Solarbio, Beijing, China) for 2 minutes. Then, the sections were blocked with 5% BSA (AR0004; Boster, Wuhan, China) for 60 minutes at room temperature and then stained with anti–NTN-1 antibody at 4°C overnight. Negative controls were incubated with the rabbit IgG isotype control antibody (1:200, ab172730; Abcam). Thereafter, the sections were incubated with fluorescein-conjugated secondary antibody for 60 minutes. All the sections were photographed using a fluorescence microscope (Olympus BX50) after counterstaining with DAPI (H-1200; Vector, Burlingame, CA, USA).

Periodic Acid–Schiff Staining

The eyeballs were fixed in 4% PFA, embedded in paraffin, and then cut into 5-µm-thick paraffin sections. The sections were then stained using a periodic acid–Schiff (PAS) staining kit (G1008-20ML; Servicebio, Wuhan, China) as per the manufacturer's instructions. The upper and lower eyelids were observed under a light microscope and photographed. Next, three sections from the central part of the eye of each mouse were stained. The number of PAS-positive cells was manually counted and averaged for each eyelid. Sections from five mice from each of the aforementioned groups were used.

Investigative Ophthalmology & Visual Science

Phenol Red Thread Test

Tear secretion was measured using the phenol red thread test at day 5 after intraperitoneal injection of 5% pentobarbital sodium (0.1 mL/10 g) under general anesthesia. A phenol red–impregnated cotton thread (AYUMI Pharmaceutical Corporation, Tokyo, Japan) was gently placed on the lateral canthus for 20 seconds for each eye with the eyes closed. The length of wetting was recorded in millimeters under the stereomicroscope.

Corneal Fluorescein Staining

One microliter of 0.25% fluorescein sodium (Jingming, Tianjin, China) was applied topically on the cornea of each eye of mice 2 hours after the last administration. After the dye was instilled, the eyes were allowed to blink several times and then were rinsed with normal saline. Corneal fluorescein staining was observed and photographed using a slit-lamp microscope (66 Vision-Tech Co. Ltd., Suzhou, China) under cobalt blue light. Corneal fluorescein staining scores were evaluated in a masked manner according to the scoring system, as described in our previous study.[31] Briefly, the cornea was separated into four quadrants, which were correspondingly scored. The four scores were summed and analyzed for each eye (minimum = 0; maximum = 16). The fluorescein score was analyzed as described previously and also as follows: positive fluorescein plaque, 4; severe diffuse staining but no positive plaque, 3; dense punctate staining with more than 30 spots, 2; slightly punctate staining with fewer than 30 spots, 1; and absent, 0.

Immunostaining of Whole-Mount Corneal Tissues

Whole-mount corneal staining was performed as described previously.[34] In brief, the mouse eyeballs were fixed in Zamboni fixative for 1 hour at 4°C. The whole corneal tissues were cut along the corneoscleral limbus and fixed in Zamboni fixed solution for 1 hour. The cornea was blocked in PBS containing 0.2% Triton X-100, 1% goat serum (Boster, AR0009), and 1% BSA (Boster) for 2 hours and subsequently incubated with primary antibodies: Alexa Fluor 488 anti–Tubulin Beta 3 Antibody (cat. 657403; Biolegend, San Diego, CA, USA) and PE-conjugated anti-mouse CD11c (Biolegend, cat. 117307). All primary antibodies were mixed in Tris-buffered saline containing 0.2% Triton X-100, 1% goat serum, and 1% BSA and incubated overnight at 4°C. The cornea was cut into six petals after washing six times, and the flat mounts were observed under a fluorescence microscope (Olympus BX50). Images of the same layer were merged to obtain an entire view of the whole-mount cornea. Innervation in central (within central 1.5 mm of the cornea) or peripheral (between 2 and 2.5 mm from the center of the cornea) regions was calculated as the percentage of area positive for β-tubulin III staining using ImageJ software (National Institutes of Health, Bethesda, MD, USA). Subsequently, the corneal DC density was calculated as the number of CD11c-positive cells in the central or peripheral regions using ImageJ software.

Flow Cytometry

The corneas with limbal tissue and submandibular and cervical draining lymph nodes (DLNs) were extracted and collected after 5 days of desiccation. Bilateral corneas with limbal tissues of two mice were polled as one sample. Excised corneas were treated with 20 µL Liberase TL (2.5 mg/mL, 5401020001; Roche, Indianapolis, IN, USA) for 30 minutes at 37°C and homogenized through a 70-µm cell strainer (BD Biosciences, Franklin Lakes, NJ, USA). The DLNs were fully ground and filtered with a 70-µm cell strainer to prepare single-cell suspensions. The cells from DLNs were stimulated with RPMI containing 50 ng/mL PMA (MB5349; Meilunbio, Dalian, China) and 500 ng/mL ionomycin (Meilunbio, MB7511) for 6 hours. Then, single-cell suspensions of cornea or DLNs were determined by flow cytometry (BD Accuri C6 Plus; BD Biosciences) using the following specific antibodies: PE/Cy5.5-conjugated anti-mouse CD86 (Biolegend, cat. 105015), PE-conjugated anti-mouse CD11c, FITC-conjugated anti-mouse CD11c (Biolegend, cat. 117305), PE-conjugated anti-mouse MHC-II (12-5322-81; eBioscience, San Diego, CA, USA), PE-conjugated anti-mouse IL-17A (Biolegend, cat. 506903), PE/Cy5.5-conjugated anti-mouse CD45 (Biolegend, cat. 103109), FITC-conjugated anti-mouse CD45 (Biolegend, cat. 157213), PE-conjugated anti-mouse CD45 (Biolegend, cat. 103106), and FITC-conjugated anti-mouse CD4 (Biolegend, cat. 100509). The negative control samples were stained with the appropriate isotype-matched antibodies. Data were analyzed using FlowJo software (Tree Star, Ashland, OR, USA).

RT-PCR

After 5 days of DED induction, tissues of the conjunctival sac, including bulbar conjunctiva and fornical conjunctiva, were collected; the conjunctivae of four eyes were pooled together as a sample. RNA was extracted using Nucleospin RNA kits (Thermo Fisher Scientific, Waltham, MA, USA) and then reverse transcribed into cDNA using the PrimeScript First-strand cDNA synthesis kit (TaKaRa, Dalian, China). RT-PCR was performed using SYBR Green reagents (R&D) and predesigned primers for IL-17A, IFN-γ, IL-1β, and IL-6. The samples were analyzed using Bio-Rad CFX Maestro1.1 (Bio-Rad Laboratories, Philadelphia, PA, USA). The quantification data were analyzed as described previously[35] using GAPDH as an internal control.

ELISA

The conjunctival proteins were extracted with cold PBS, and a BCA protein assay kit (ZJ102; Epizyme, Shanghai, China) was used to measure the total protein concentration; the conjunctivae of four eyes were pooled together as a sample. IFN-γ (cat. m1002277-C; Mlbio, Shanghai, China) and IL-17 (Mlbio, cat. m1037864-C) levels in the conjunctiva were quantified as per the manufacturer's instructions of the ELISA kits. Optical absorbance was measured at 450 nm using a microplate reader (C_{Max} Plus; Molecular Devices, San Francisco, CA, USA), and the protein concentration of each sample was measured using a standard curve.

Statistical Analyses

All statistical analyses were performed using GraphPad Prism software (version 8.0; GraphPad Software, La Jolla, CA, USA). Student's *t*-test was used to compare two groups, and one-way analysis of variance was used to compare more than three groups. Data are shown as mean ± SEM. The difference was considered significant at $P < 0.05$.

Results

Transcriptome Analysis of Corneal Epithelium of DED and Control Mice

The corneal epithelium of DED mice and age- and sex-matched healthy control mice was subjected to an RNA sequencing study ($n = 3$). The volcano plot (Fig. 1A) showed the DEGs between the two groups. A total of 292 genes were markedly upregulated (including VEGFa, NGFR, VIPR1, TAC-1, etc.) and 55 genes were markedly downregulated (including NTN-1 and SLIT2) in the DED group compared with the control group. KEGG pathway analysis was performed for all DEGs, and the top 20 KEGG categories are displayed in Figure 1B. Hierarchical clustering analysis (Fig. 1C) showed distinct expression profiles between the corneal epithelium of the DED group and the control group.

Expression of NTN-1 Derived From Corneal Epithelium Decreases in DED Mice

To study the change in expression of NTN-1 in DED, we collected corneal epithelium from the control mice and DED mice after 3 and 5 days of desiccation. Sequencing analysis of the corneal epithelium of DED and control mice indicated that the expression of NTN-1 was decreased in the corneal epithelium of the DED mice (Fig. 2A). Real-time PCR results showed that the mRNA expression of NTN-1 was decreased by 64.33% ($P < 0.001$) in the corneal epithelium of the DED mice after 5 days of induction compared with that in the normal mice. However, no difference was found in the corneal epithelium of the normal mice and DED mice 3 days after induction (Fig. 2B). In agreement with the changes observed in the gene expression levels, the Western blotting analysis results also revealed that the protein level of NTN-1 in the corneal epithelium of the DED mice was lower than that in the normal mice (Figs. 2C, 2D). Furthermore, immunofluorescent staining of frozen corneal sections also confirmed a significant decrease in the protein expression of NTN-1 in the DED mice compared to control (Fig. 2E).

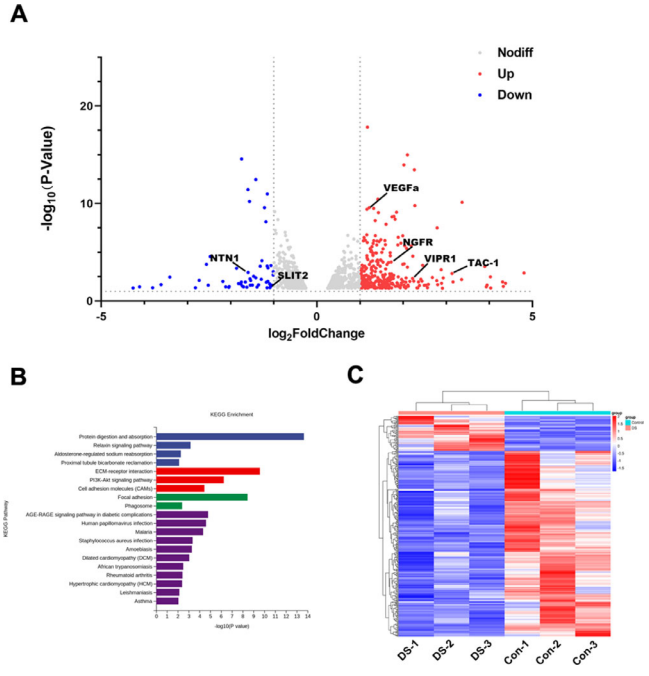

Figure 1. Analyses of DEGs between corneal epithelium of DED and normal mice. (**A**) The volcano plot represents the DEGs between corneal epithelium of DED and normal mice: *red* indicates upregulated and *blue* indicates downregulated. (**B**) Enrichment of KEGG pathways in corneal epithelium of DED mice compared to normal mice. (**C**) Heatmap generated from a hierarchical cluster analysis, illustrating the different expression profiling between corneal epithelium of DED and normal mice. The corneal epithelium of four eyes was pooled together as a sample, $n = 3$ per group. Control, corneal epithelium of normal mice. DS, corneal epithelium of DED mice.

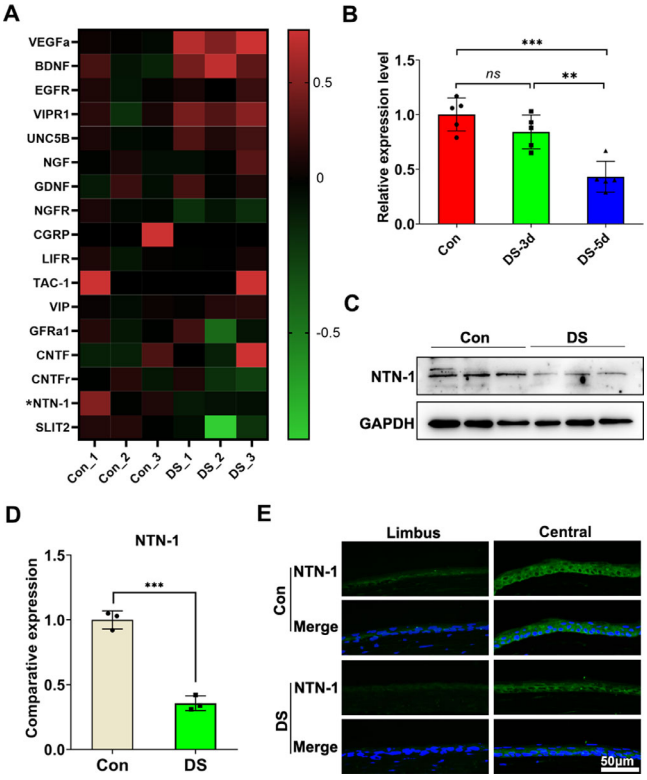

Figure 2. Expression of NTN-1 derived by corneal epithelium decreases in DED mice. (**A**) Heatmap identified differentially expressed neural factors in corneal epithelium of DED mice and normal mice detected using RNA-seq. (**B**) The mRNA levels of NTN-1 by the corneal epithelial were quantified using real-time PCR (corneal epithelium was collected on day 3 or day 5 post-DED induction; the corneal epithelium of four eyes was pooled together as a sample, $n = 5$). (**C**, **D**) The protein levels of NTN-1 in the corneal epithelium were evaluated by Western blot, with GAPDH as the internal control (corneal epithelium was collected on day 5 after DED induction; the corneal epithelium of four eyes was pooled together as a sample, $n = 3$). (**E**) Representative images of corneal NTN-1 immunofluorescence staining. Three independent experiments were pooled in the statistical analysis. Data are shown as mean ± SEM. $^{**}P < 0.01$, $^{***}P < 0.001$. ns, no significance.

Topical NTN-1 Reduces the Severity of DED

During DED induction, the mice were treated with PBS (desiccating stress [DS] group) or recombinant mouse NTN-1 (25 ng/5 μL; DS + NTN-1 group) for 5 days. To investigate the efficacy of exogenous NTN-1 on ocular surface injury, we evaluated corneal epithelial injury, tear secretion, and goblet cell density in the DED mouse model. The corneal fluorescein score in the DS group (12.50 ± 1.20 vs. 0.50 ± 0.67; $P <$

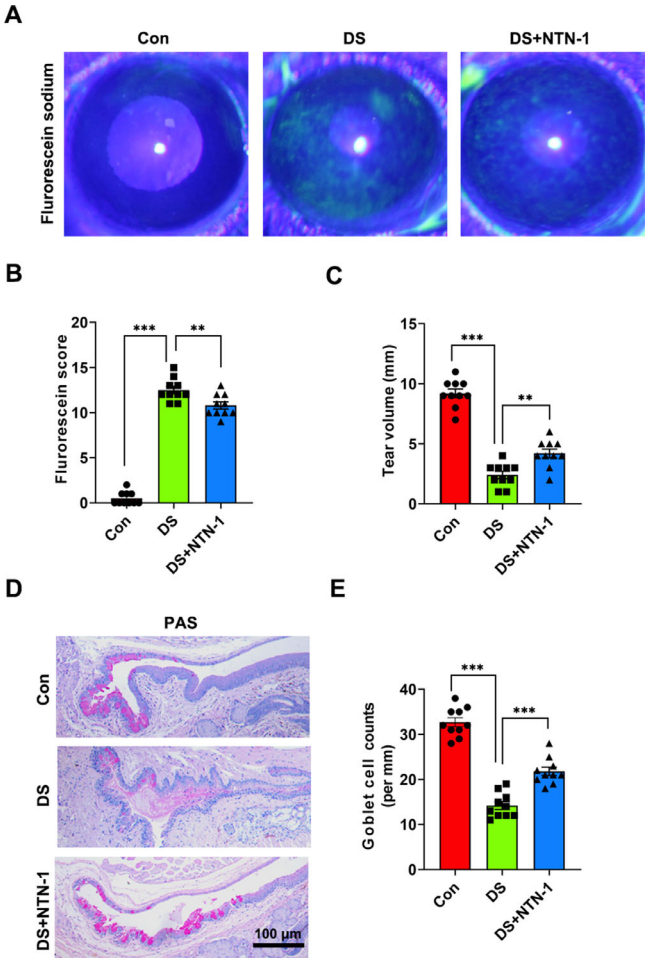

Figure 3. Topical NTN-1 treatment alleviated the damage of DED. (**A**) Representative photos of cornea fluorescein sodium staining in each group. (**B**) The score of corneal fluorescein sodium staining. (**C**) Phenol red thread test for the quantification of tear volume. (**D**) Representative photos of PAS staining in conjunctiva. (**E**) PAS-positive cells were manually counted and averaged from each eyelid for each group. $n = 5$ mice per group. Three independent experiments were pooled in the statistical analysis. Data are shown as mean ± SEM. $^{**}P < 0.01$, $^{***}P < 0.001$.

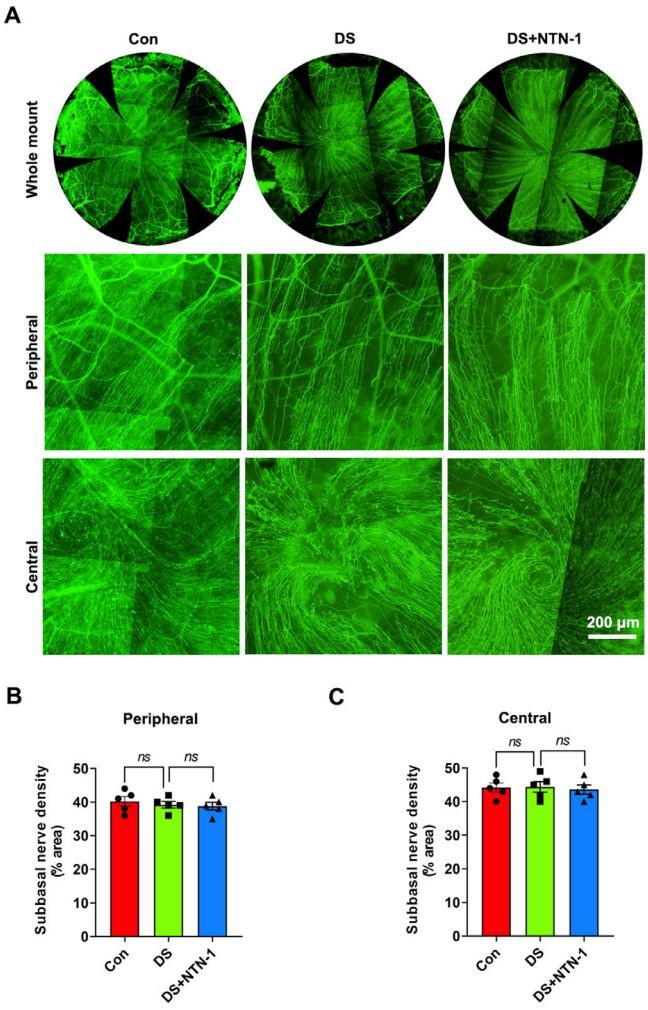

Figure 4. Alterations of corneal nerves in DED. (**A**) Corneal nerves were stained for β-tubulin III. *Upper panels* are images of whole corneal nerves, *middle panels* are peripheral corneal nerve images, and *lower panels* are central corneal nerve images. (**B**, **C**) Nerve density in the peripheral cornea or central cornea was calculated from the staining positive area using ImageJ software ($n = 5$). Three independent experiments were pooled in the statistical analysis. Data are shown as mean ± SEM.

0.001) was higher than that in the control group. However, treatment with topical NTN-1 (10.80 ± 1.17 vs. 12.50 ± 1.20; $P < 0.01$) reduced this score (Figs. 3A, 3B). Phenol red thread test showed that compared to the control group, tear production in the DS group (2.40 ± 0.92 vs. 9.20 ± 1.08 mm; $P <$ 0.001) was significantly reduced but was increased in the DS + NTN-1 group (4.20 ± 1.08 vs. 2.40 ± 0.92 mm; $P <$ 0.01). In addition, the number of PAS-stained goblet cells in the conjunctiva was decreased in the DS group (14.20 ± 2.60 vs. 32.70 ± 3.03; $P < 0.001$), whereas the number of conjunctival goblet cells treated with NTN-1 (21.80 ± 2.79 vs. 14.20 ± 2.60; $P < 0.001$) was increased significantly (Figs. 3D, 3E).

Density of Corneal Sensory Nerve Fibers and Terminals Did Not Change in DED

To explore the changes in the corneal nerves in DED mice, we performed immunostaining of whole-mount corneal tissues in the control, DS, and DS + NTN-1 groups. Compared with the intact morphology of the corneal nerve fibers in the control group, we observed no differences in the corneal nerve fiber morphology between the DS and DS + NTN-1 groups (Fig. 4A). Moreover, the density of nerve fiber terminals in central (within central 1.5 mm of the cornea) or peripheral (between 2 and 2.5 mm from the center of the cornea) regions of the cornea in the DS and DS + NTN-1 groups was not significant when compared to the control group (Figs. 4B, 4C).

Topical NTN-1 Inhibits the Activation of Corneal Epithelial DCs in DED

CD11c staining was performed to evaluate DC population in the corneal epithelium. The staining results showed that the number of DCs in the corneal epithelium in the DS group was higher than that in the control group, whereas the number of DCs in the DS + NTN-1 group was significantly lower than that in the DS group (Fig. 5A). The assessment of corneal central and peripheral DC density demonstrated

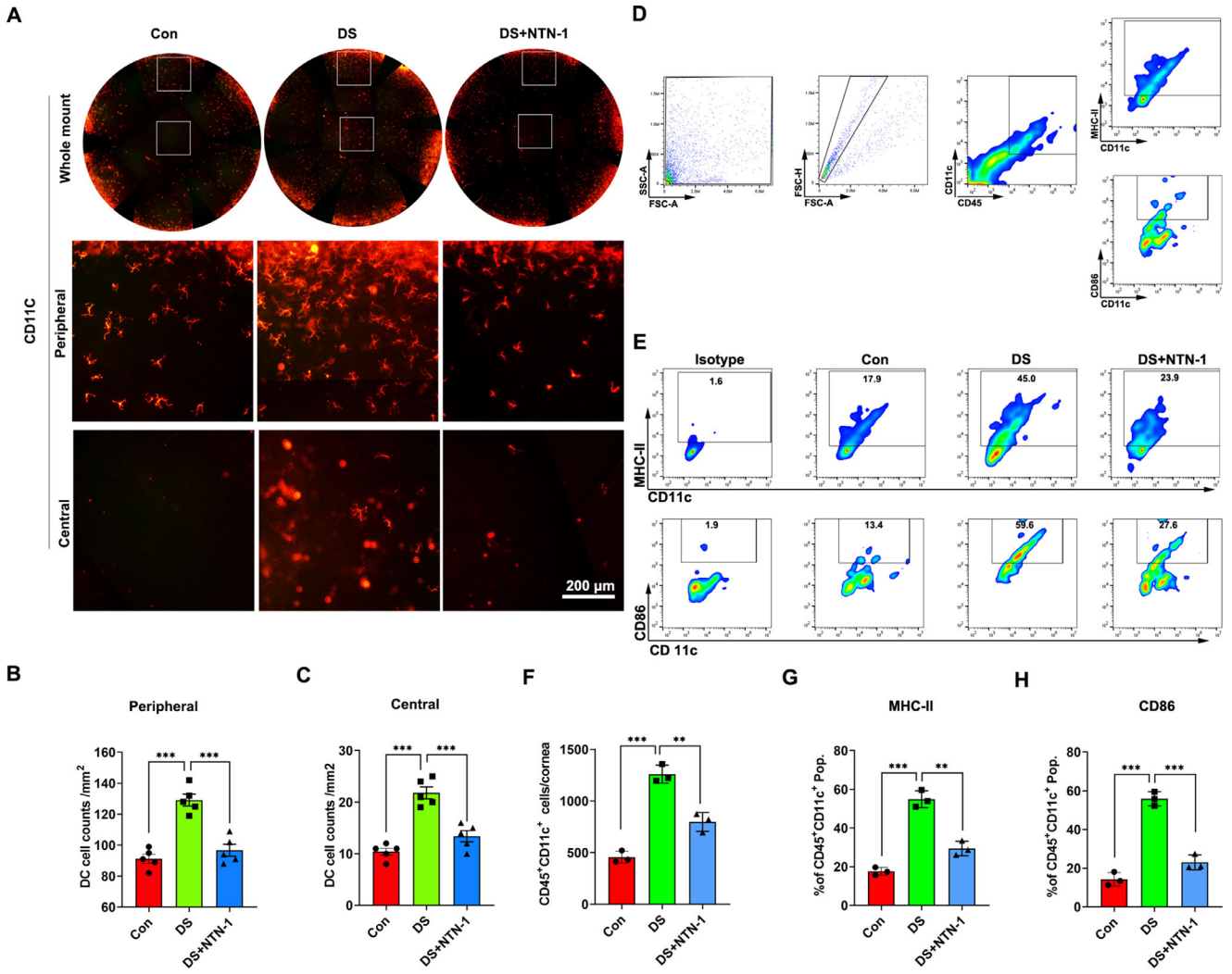

Figure 5. Topical NTN-1 reduces the density of corneal epithelial DCs in DED. (**A**) DCs of corneal epithelium were stained for CD11c. *Upper panels* are images of whole corneal DCs, *middle panels* are peripheral corneal DCs images, and *lower panels* are central corneal DCs images. (**B**, **C**) DC density in the peripheral cornea or central cornea was calculated from the staining positive area using ImageJ software ($n = 5$). (**D**) Single-cell preparations from cornea were prepared and analyzed by flow cytometry. The gating strategies are justified by appropriate isotype control antibodies. (**E**) Representative flow cytometry plots of $CD11c^+MHC\text{-}II^+$ DCs and $CD11c^+CD86^+$ DCs in the cornea (corneas with limbal tissue of two mice were polled as one sample). (**F**) The number of $CD45^+CD11c^+$ DCs in cornea. (**G**) Frequencies of $MHC\text{-}II^+$ DCs in cornea. (**H**) Frequencies of $CD86^+$ DCs in cornea. Three independent experiments were pooled in the statistical analysis. Data are shown as mean ± SEM. $^{**}P < 0.01$, $^{***}P < 0.001$.

a strong correlation between the three groups (Figs. 5B, 5C). Furthermore, flow cytometric data also revealed that the number of $CD45^+CD11c^+$ cells in cornea was increased in the DS group, whereas it was significantly reduced in the DS + NTN-1 group. Moreover, the frequency of $MHC\text{-}II^+$ DCs and $CD86^+$ DCs in the cornea in the DS group was higher than that in the control group, whereas the frequency of these two cells was significantly lower in the DS + NTN-1 group (Figs. 5D–H).

Topical NTN-1 Reduces Th17 Immune Response Mediated by Activated DCs in DED

To explore the effect of NTN-1 on the immune response mediated by activated DCs in DED, DLNs and conjunctivae of the mice were analyzed by flow cytometry and RT-PCR, respectively, after 5 days of desiccation. Flow cytometric data revealed that the frequency of $CD11c^+CD86^+$ DCs, $CD11c^+MHC\text{-}II^+$ DCs, and $CD4^+IL\text{-}17A^+$ cells in the DLNs in the DS group was higher than that in the control group, whereas the frequency of these two cells was significantly lower in the DS + NTN-1 group (Figs. 6A–E). Moreover, RT-PCR data showed that the mRNA expression levels of inflammatory cytokines IL-17, IFN- γ, IL-1β, and IL-6 in the conjunctiva of mice in the DS + NTN-1 group were significantly decreased compared to DED mice (Figs. 6F–I). Moreover, the protein levels of IL-17 and IFN-γ in the conjunctiva of DS + NTN-1–treated mice were also significantly decreased compared to DED mice (Figs. 6J–K).

NTN-1 Neutralizing Antibody Exacerbated Inflammation in DED

During DED induction, the mice were treated with goat IgG (DS + IgG group) or anti-mouse NTN-1 antibody (DS + αNTN-1 antibody [Ab] group) for 5 days. Corneal fluorescein

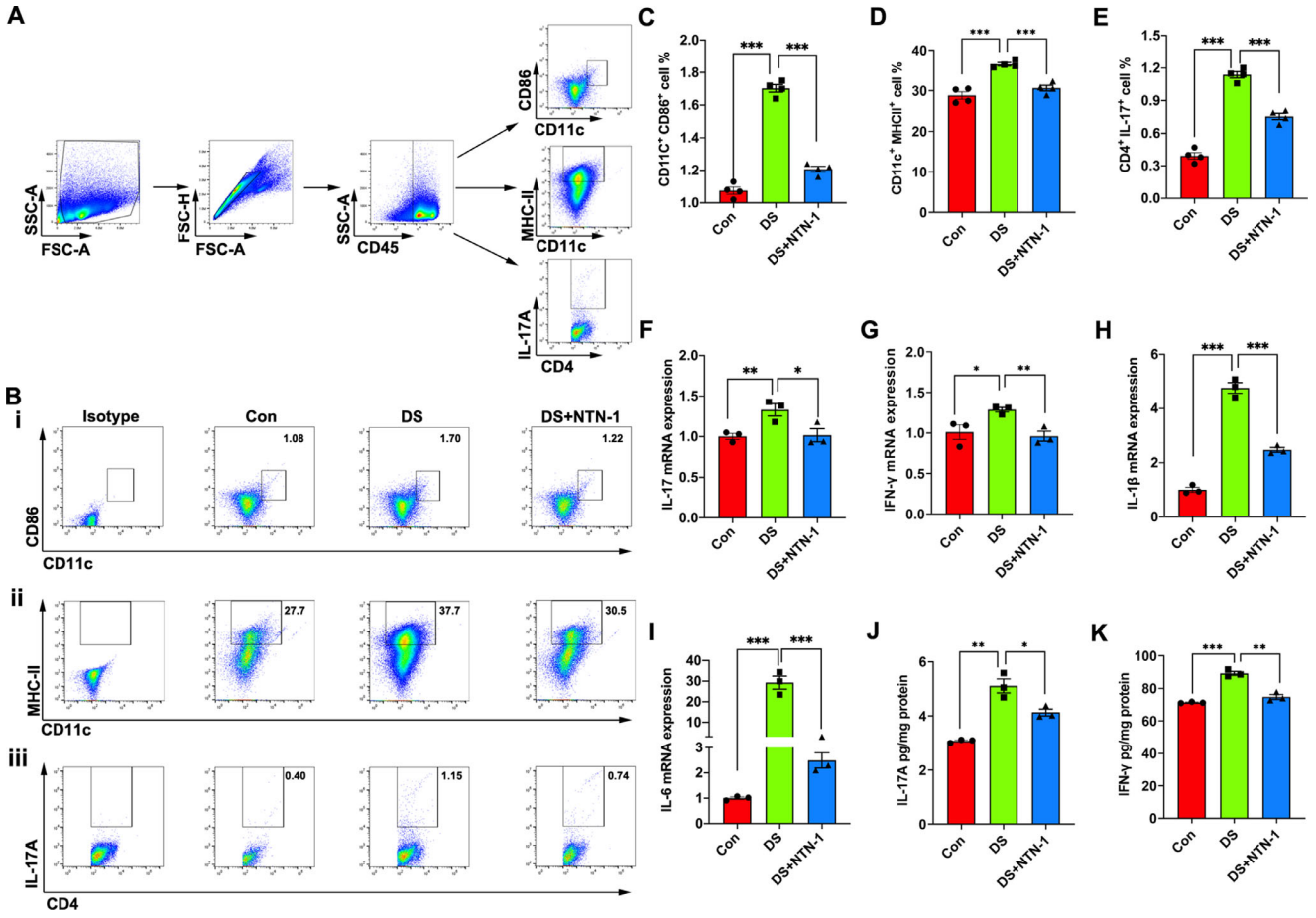

Figure 6. Topical NTN-1 reduces Th17 immune response mediated by activated DCs in DED. (**A**) Single-cell preparations from DLNs were prepared and analyzed by flow cytometry. The gating strategies are justified by appropriate isotype control antibodies. (**B**) Representative flow cytometry plots of $CD11c^+CD86^+$ DCs (i), $CD11c^+MHC\text{-}II^+$ DCs (ii), and $IL\text{-}17^+CD4^+$ T cells (iii) in the DLNs. (**C**) Frequencies of $CD11c^+CD86^+$ DCs in the DLNs ($n = 4$ mice). (**D**) Frequencies of $CD11c^+MHC\text{-}II^+$ DCs in the DLNs ($n = 4$ mice). (**E**) Frequencies of $IL\text{-}17^+CD4^+$ T cells in the DLNs ($n = 4$ mice). (**F–I**) mRNA expression levels of Th17-related genes in conjunctiva (the conjunctiva tissues of four eyes were pooled together as a sample; $n = 3$). (**J–K**) Protein expression levels of Th17-related genes in conjunctiva (the conjunctiva tissues of four eyes were pooled together as a sample; $n = 3$). Three independent experiments were pooled in the statistical analysis. Data are shown as mean ± SEM. $^*P < 0.05$, $^{**}P < 0.01$, $^{***}P < 0.001$.

sodium staining showed that corneal epithelial defects were more severe in the DS + αNTN-1 Ab group than in the DS + IgG group (Fig. 7A), and the corneal fluorescein staining scores were higher (Fig. 7B). In addition, tear secretion was reduced in mice in the DS + αNTN-1 Ab group compared with the DS + IgG group (Fig. 7C). The density of DCs in the central and peripheral regions of the cornea was higher in the DS + αNTN-1 Ab group than in the DS + IgG group (Figs. 7D, 7E). Furthermore, the frequency of Th17 cells in the DLNs of the mice in the DS + αNTN-1 Ab group was higher than that in the DS + IgG group (Fig. 7F).

Discussion

DED is an autoimmune-mediated inflammatory disease of the ocular surface.[1] The corneal epithelium not only defends against external injury and infection but also plays a key role in regulating the immune responses at the ocular surface.[3,36] In the present study, we demonstrated that corneal epithelium–derived NTN-1 expression was decreased in DED mice. Furthermore, we demonstrated that in a DED mouse model, NTN-1 reduced the severity of dry eye and exerted its anti-inflammatory effect by inhibiting DC activation, thereby inhibiting Th17 cell-mediated inflammatory responses.

The immune response in DED reflects the balance between proinflammatory and anti-inflammatory factors on the ocular surface. The corneal epithelium secretes various immunomodulatory factors such as PD-L1, PEDF, TSP-1, and NTN-1 to regulate ocular surface inflammation. In DED, TSP-1[37] and PEDF[38] expression levels were upregulated, but PD-L1[20] expression was downregulated, indicating that different immunomodulatory factors may increase or decrease in DED. Our study showed that the expression of NTN-1 in the corneal epithelium decreased in the DED mice. This result implies that decreased NTN-1 expression might result in the initiation and progression of DED. Indeed, NTN-1 not only is a traditional guiding clue for the growth of axons in the nervous system but also has the function of regulating inflammatory response,[24] which has been confirmed in several ocular diseases. In the mouse model of *Aspergillus fumigatus* keratitis, NTN-1 inhibits the inflammatory response through the A2BAR receptor.[29] In the diabetic mouse model, topical NTN-1 treatment

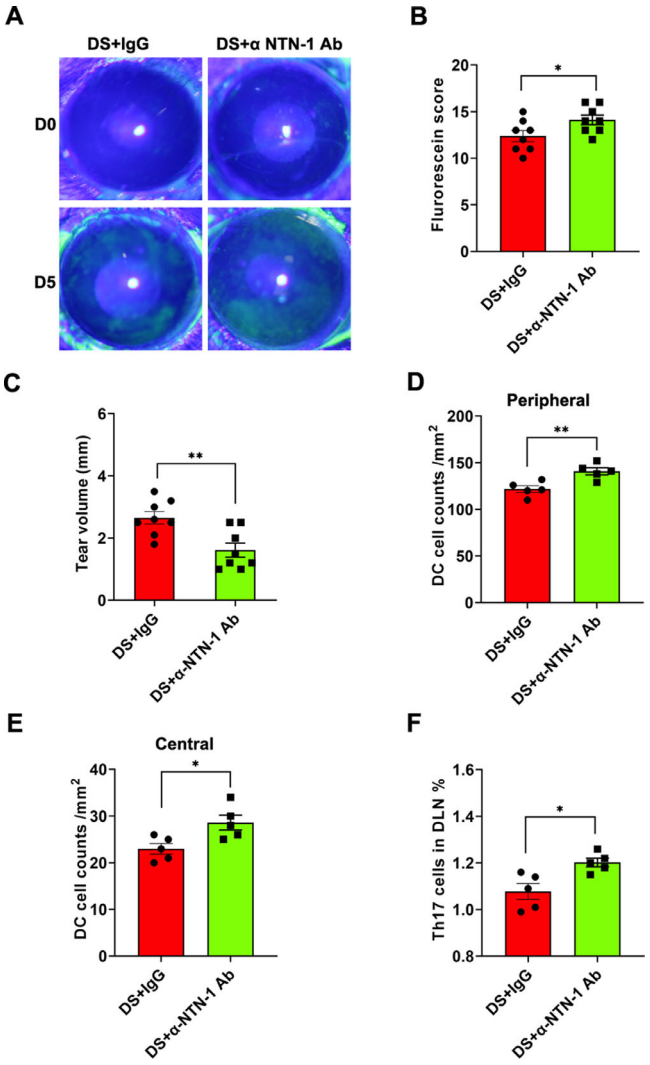

Figure 7. NTN-1 neutralizing antibody exacerbated inflammation in DED. (**A**) Representative photos of cornea fluorescein sodium staining in each group. (**B**) The score of corneal fluorescein sodium staining ($n = 4$ mice). (**C**) Schirmer's test for the quantification of tear volume ($n = 4$ mice). (**D**, **E**) DC density in the peripheral cornea or central cornea was calculated from the staining positive area using ImageJ software ($n = 5$). (**F**) Frequencies of Th17 cells in the DLNs ($n = 5$ mice). Three independent experiments were pooled in the statistical analysis. Data are shown as mean ± SEM. $^{*}P < 0.05$, $^{**}P < 0.01$.

promotes wound healing of the diabetic corneal epithelium, inhibits neutrophil infiltration, and induces M2 polarization of macrophages.[30] In the rat model with corneal alkali burn, NTN-1 application not only inhibited and reversed corneal neovascularization but also reduced corneal inflammatory response.[28]

To further investigate the therapeutic effects of NTN-1 in DED, we topically applied recombinant NTN-1 to DED mice. Our DED mouse model is based on a well-established paradigm that uses low humidity airflow and simultaneous administration of scopolamine to induce dry eye in mice to produce ocular surface epithelial changes similar to human DED.[39] Our results showed that the punctate defect of corneal epithelium in the treatment group was reduced, suggesting that NTN-1 protects the integrity of corneal epithelium and maintains its barrier effect. In addition, goblet cells in the conjunctiva can secrete mucin, which is essential to maintain tear film stability. Our results showed that topical application of NTN-1 restored the number of goblet cells in conjunctiva and reduced the expression of IL-17, IFN-γ, and other inflammatory factors in conjunctiva, suggesting that NTN-1 may play a therapeutic role by inhibiting the inflammatory response on the ocular surface.

As one of the most innervated tissues, the corneal nerves play an important role in the homeostasis of the ocular surface environment by performing nerve reflex and secreting a variety of neuropeptides essential for the maintenance of epithelial cells and stromal cells.[40,41] However, there are conflicting results regarding the changes in the corneal nerve fiber density (CNFD) in DED.[42] Some studies reported a decrease in CNFD in DED,[43] whereas others reported no difference or a significant increase in CNFD in DED.[44–47] Our data showed that there was no significant difference in the CNFD between the three experimental groups, suggesting that NTN-1 may not play a therapeutic role in DED by affecting the corneal nerve density.

The change in the number of DCs in the cornea is a potential biological marker of DED.[48] DCs, as an APC, play an important role in DED pathogenesis.[49] In normal corneas, DCs are mostly located around the peripheral region. In case of DED, the DCs undergo a series of changes such that they are activated in response to an inflammatory response. These changes include an increase in the quantity, change in location (migration from the periphery to the center of the cornea), and an increase in the expression of surface markers (MHC-II, CD86, etc.).[50,51] Through in vivo experiments, we proved that after topical application of recombinant NTN-1, the number of corneal DCs and the frequency of $CD11c^{+}CD86^{+}$ DCs decreased significantly, confirming the inhibitory effect of NTN-1 on DC activation.

Studies have shown migration to the submandibular and cervical DLNs after cellular activation of DCs in DED.[3,52] After reaching the DLNs, the presentation of ocular surface antigens by DCs promotes the differentiation of naive T cells, leading to the generation of effector T-cell subsets that are dominated by the Th17 cells.[10,52,53] Our study showed that after blocking corneal epithelium–derived NTN-1 with an anti–NTN-1 antibody, the activation of DCs in the cornea significantly increased, the frequency of Th17 cells in the DLNs increased, and the expression of proinflammatory factors in the conjunctiva was elevated. In contrast, topical recombinant NTN-1 exerted a significant effect in suppressing DC activation in the cornea, persisting Th17 cell generation, and suppressing the expression of proinflammatory factors on the ocular surface.

The limitations of our study must be acknowledged. First, our experiments confirmed that NTN-1 can inhibit the activation of DCs; however, the specific mechanism by which NTN-1 inhibits the activation of DCs remains unclear. Second, our experimental results were not validated in in vitro experiments.

In conclusion, we found that corneal epithelium–derived NTN-1 expression was reduced in DED. Additionally, our findings suggested that NTN-1 exerted anti-inflammatory effects by inhibiting DCs activation-mediated Th17 immune responses, thereby alleviating corneal epithelial injury in DED. As an endogenous protein secreted by the corneal epithelium, NTN-1 modulation may be a novel therapeutic approach for patients with DED.

Investigative Ophthalmology & Visual Science

Acknowledgments

The authors thank Editage for its linguistic assistance during the preparation of this manuscript.

Supported by the National Natural Science Foundation of China (Nos. 81670829 and 81970782) and the China Postdoctoral Science Foundation (No. 2019M652328).

Disclosure: **C. Yu,** None; **P. Chen,** None; **J. Xu,** None; **S. Wei,** None; **Q. Cao,** None; **C. Guo,** None; **X. Wu,** None; **G. Di,** None

References

1. Craig JP, Nichols KK, Akpek EK, et al. TFOS DEWS II definition and classification report. *Ocul Surf*. 2017;15:276–283.
2. Dai Y, Zhang J, Xiang J, Li Y, Wu D, Xu J. Calcitriol inhibits ROS-NLRP3-IL-1β signaling axis via activation of Nrf2-antioxidant signaling in hyperosmotic stress stimulated human corneal epithelial cells. *Redox Biol*. 2019;21:101093.
3. Barabino S, Chen Y, Chauhan S, Dana R. Ocular surface immunity: homeostatic mechanisms and their disruption in dry eye disease. *Prog Retin Eye Res*. 2012;31:271–285.
4. Giusto E, Donegà M, Cossetti C, Pluchino S. Neuro-immune interactions of neural stem cell transplants: from animal disease models to human trials. *Exp Neurol*. 2014;260:19–32.
5. Clark AK, Malcangio M. Fractalkine/CX3CR1 signaling during neuropathic pain. *Front Cell Neurosci*. 2014;8:121.
6. Knickelbein JE, Watkins SC, McMenamin PG, Hendricks RL. Stratification of antigen-presenting cells within the normal cornea. *Ophthalmol Eye Dis*. 2009;1:45–54.
7. Bereiter DA, Rahman M, Thompson R, Stephenson P, Saito H. TRPV1 and TRPM8 channels and nocifensive behavior in a rat model for dry eye. *Invest Ophthalmol Vis Sci*. 2018;59:3739–3746.
8. Gao N, Lee P, Yu FS. Intraepithelial dendritic cells and sensory nerves are structurally associated and functional interdependent in the cornea. *Sci Rep*. 2016;6:36414.
9. Pennock ND, White JT, Cross EW, Cheney EE, Tamburini BA, Kedl RM. T cell responses: naive to memory and everything in between. *Adv Physiol Educ*. 2013;37:273–283.
10. Yu M, Lee SM, Lee H, et al. Neurokinin-1 receptor antagonism ameliorates dry eye disease by inhibiting antigen-presenting cell maturation and T helper 17 cell activation. *Am J Pathol*. 2020;190:125–133.
11. Luckheeram RV, Zhou R, Verma AD, Xia B. $CD4^+$T cells: differentiation and functions. *Clin Dev Immunol*. 2012;2012:925135.
12. Pflugfelder SC, Corrales RM, de Paiva CS. T helper cytokines in dry eye disease. *Exp Eye Res*. 2013;117:118–125.
13. De Paiva CS, Chotikavanich S, Pangelinan SB, et al. IL-17 disrupts corneal barrier following desiccating stress. *Mucosal Immunol*. 2009;2:243–253.
14. Fan NW, Dohlman TH, Foulsham W, et al. The role of Th17 immunity in chronic ocular surface disorders. *Ocul Surf*. 2021;19:157–168.
15. Chen Y, Dana R. Autoimmunity in dry eye disease—An updated review of evidence on effector and memory Th17 cells in disease pathogenicity. *Autoimmun Rev*. 2021;20:102933.
16. Zhang X, Schaumburg CS, Coursey TG, et al. $CD8^+$ cells regulate the T helper-17 response in an experimental murine model of Sjögren syndrome. *Mucosal Immunol*. 2014;7:417–427.
17. Chauhan SK, Dana R. Role of Th17 cells in the immunopathogenesis of dry eye disease. *Mucosal Immunol*. 2009;2:375–376.
18. Liu R, Gao C, Chen H, Li Y, Jin Y, Qi H. Analysis of Th17-associated cytokines and clinical correlations in patients with dry eye disease. *PLoS One*. 2017;12:e0173301.
19. Ma B, Zhou Y, Liu R, et al. Pigment epithelium-derived factor (PEDF) plays anti-inflammatory roles in the pathogenesis of dry eye disease. *Ocul Surf*. 2021;20:70–85.
20. El Annan J, Goyal S, Zhang Q, Freeman GJ, Sharpe AH, Dana R. Regulation of T-cell chemotaxis by programmed death-ligand 1 (PD-L1) in dry eye-associated corneal inflammation. *Invest Ophthalmol Vis Sci*. 2010;51:3418–3423.
21. Kenchegowda S, He J, Bazan HE. Involvement of pigment epithelium-derived factor, docosahexaenoic acid and neuroprotectin D1 in corneal inflammation and nerve integrity after refractive surgery. *Prostaglandins Leukot Essent Fatty Acids*. 2013;88:27–31.
22. Tan X, Chen Y, Foulsham W, et al. The immunoregulatory role of corneal epithelium-derived thrombospondin-1 in dry eye disease. *Ocul Surf*. 2018;16:470–477.
23. Serafini T, Kennedy TE, Galko MJ, Mirzayan C, Jessell TM, Tessier-Lavigne M. The netrins define a family of axon outgrowth-promoting proteins homologous to C. elegans UNC-6. *Cell*. 1994;78:409–424.
24. Ly NP, Komatsuzaki K, Fraser IP, et al. Netrin-1 inhibits leukocyte migration in vitro and in vivo. *Proc Natl Acad Sci USA*. 2005;102:14729–14734.
25. Mirakaj V, Gatidou D, Pötzsch C, König K, Rosenberger P. Netrin-1 signaling dampens inflammatory peritonitis. *J Immunol*. 2011;186:549–555.
26. Aherne CM, Collins CB, Masterson JC, et al. Neuronal guidance molecule netrin-1 attenuates inflammatory cell trafficking during acute experimental colitis. *Gut*. 2012;61:695–705.
27. Mirakaj V, Thix CA, Laucher S, et al. Netrin-1 dampens pulmonary inflammation during acute lung injury. *Am J Respir Crit Care Med*. 2010;181:815–824.
28. Han Y, Shao Y, Lin Z, et al. Netrin-1 simultaneously suppresses corneal inflammation and neovascularization. *Invest Ophthalmol Vis Sci*. 2012;53:1285–1295.
29. Zhou Y, Lin J, Peng X, et al. The role of netrin-1 in the mouse cornea during *Aspergillus fumigatus* infection. *Int Immunopharmacol*. 2019;71:372–381.
30. Zhang Y, Chen P, Di G, Qi X, Zhou Q, Gao H. Netrin-1 promotes diabetic corneal wound healing through molecular mechanisms mediated via the adenosine 2B receptor. *Sci Rep*. 2018;8:5994.
31. Yu C, Chen P, Xu J, et al. hADSCs derived extracellular vesicles inhibit NLRP3inflammasome activation and dry eye. *Sci Rep*. 2020;10:14521.
32. Yu C, Chen H, Qi X, Chen P, Di G. Annexin A1 mimetic peptide Ac2-26 attenuates mechanical injury induced corneal scarring and inflammation. *Biochem Biophys Res Commun*. 2019;519:396–401.
33. Di GH, Qi X, Xu J, et al. Therapeutic effect of secretome from TNF-α stimulated mesenchymal stem cells in an experimental model of corneal limbal stem cell deficiency. *Int J Ophthalmol*. 2021;14:179–185.
34. Liu Y, Di G, Wang Y, Chong D, Cao X, Chen P. AQP5 facilitates corneal epithelial wound healing and nerve regeneration by reactivating Akt signaling pathway. *Am J Pathol*. 2021;191:1974–1985.
35. Liu Y, Di G, Hu S, et al. Expression profiles of CircRNA and mRNA in lacrimal glands of AQP5(–/–) mice with primary dry eye. *Front Physiol*. 2020;11:1010.
36. Pflugfelder SC, de Paiva CS, Li DQ, Stern ME. Epithelial-immune cell interaction in dry eye. *Cornea*. 2008;27(suppl 1):S9–S11.
37. Foulsham W, Dohlman TH, Mittal SK, et al. Thrombospondin-1 in ocular surface health and disease. *Ocul Surf*. 2019;17:374–383.

Investigative Ophthalmology & Visual Science

38. Singh RB, Blanco T, Mittal SK, et al. Pigment Epithelium-derived factor secreted by corneal epithelial cells regulates dendritic cell maturation in dry eye disease. *Ocul Surf*. 2020;18:460–469.
39. Dursun D, Wang M, Monroy D, et al. A mouse model of keratoconjunctivitis sicca. *Invest Ophthalmol Vis Sci*. 2002;43:632–638.
40. Ferrari G, Chauhan SK, Ueno H, et al. A novel mouse model for neurotrophic keratopathy: trigeminal nerve stereotactic electrolysis through the brain. *Invest Ophthalmol Vis Sci*. 2011;52:2532–2539.
41. Ueno H, Ferrari G, Hattori T, et al. Dependence of corneal stem/progenitor cells on ocular surface innervation. *Invest Ophthalmol Vis Sci*. 2012;53:867–872.
42. Xu J, Chen P, Yu C, Liu Y, Hu S, Di G. In vivo confocal microscopic evaluation of corneal dendritic cell density and subbasal nerve parameters in dry eye patients: a systematic review and meta-analysis. *Front Med*. 2021;8:578233.
43. Zhang M, Chen J, Luo L, Xiao Q, Sun M, Liu Z. Altered corneal nerves in aqueous tear deficiency viewed by in vivo confocal microscopy. *Cornea*. 2005;24:818–824.
44. Tuominen IS, Konttinen YT, Vesaluoma MH, Moilanen JA, Helintö M, Tervo TM. Corneal innervation and morphology in primary Sjögren's syndrome. *Invest Ophthalmol Vis Sci*. 2003;44:2545–2549.
45. Labbé A, Liang Q, Wang Z, et al. Corneal nerve structure and function in patients with non-Sjogren dry eye: clinical correlations. *Invest Ophthalmol Vis Sci*. 2013;54:5144–5150.
46. Hoşal BM, Ornek N, Zilelioğlu G, Elhan AH. Morphology of corneal nerves and corneal sensation in dry eye: a preliminary study. *Eye*. 2005;19:1276–1279.
47. Erdélyi B, Kraak R, Zhivov A, Guthoff R, Németh J. In vivo confocal laser scanning microscopy of the cornea in dry eye. *Graefes Arch Clin Exp Ophthalmol*. 2007;245:39–44.
48. Senthil K, Jiao H, Downie LE, Chinnery HR. Altered corneal epithelial dendritic cell morphology and phenotype following acute exposure to hyperosmolar saline. *Invest Ophthalmol Vis Sci*. 2021;62:38.
49. Oh J, Shin JS. The role of dendritic cells in central tolerance. *Immune Netw*. 2015;15:111–120.
50. Jiao H, Naranjo Golborne C, Dando SJ, McMenamin PG, Downie LE, Chinnery HR. Topographical and morphological differences of corneal dendritic cells during steady state and inflammation. *Ocul Immunol Inflamm*. 2020;28:898–907.
51. Levine H, Hwang J, Dermer H, Mehra D, Feuer W, Galor A. Relationships between activated dendritic cells and dry eye symptoms and signs. *Ocul Surf*. 2021;21:186–192.
52. Maruoka S, Inaba M, Ogata N. Activation of dendritic cells in dry eye mouse model. *Invest Ophthalmol Vis Sci*. 2018;59:3269–3277.
53. Ouyang W, Wu Y, Lin X, et al. Role of CD4+ T helper cells in the development of BAC-induced dry eye syndrome in mice. *Invest Ophthalmol Vis Sci*. 2021;62:25.